



Since January 2020 Elsevier has created a COVID-19 resource centre with free information in English and Mandarin on the novel coronavirus COVID-19. The COVID-19 resource centre is hosted on Elsevier Connect, the company's public news and information website.

Elsevier hereby grants permission to make all its COVID-19-related research that is available on the COVID-19 resource centre - including this research content - immediately available in PubMed Central and other publicly funded repositories, such as the WHO COVID database with rights for unrestricted research re-use and analyses in any form or by any means with acknowledgement of the original source. These permissions are granted for free by Elsevier for as long as the COVID-19 resource centre remains active.

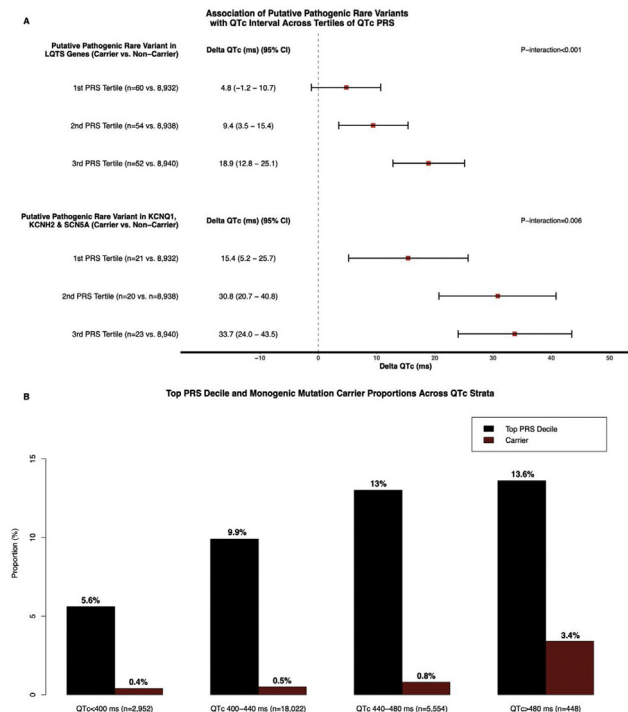


Figure 1. A. Multivariate Association of Putative Pathogenic Rare Variant Carrier Status with QTc Interval Across Tertiles of QTc Polygenic Risk Score. B. Top PRS Decile and Monogenic Mutation Carrier Proportions Across QTc Strata. Multivariate models were adjusted for age, sex, beta-blocker therapy, sodium channel blocker therapy and first 13 principal components. Interaction analysis was performed by including an interaction term (top tertile * carrier status) in the multivariate model. LQTS: Long QT Syndrome; PRS: Polygenic Risk Score; LQTS genes included KCNQ1, KCNH2, SCN5A, KCNJ2, KCNE2, CACNA1C, CACNA2D1, CACNA2D2, CACNA2D3, CACNA2D4, CACNA2D5, CACNA2D6, CACNA2D7, CACNA2D8, CACNA2D9, CACNA2D10, CACNA2D11, CACNA2D12, CACNA2D13, CACNA2D14, CACNA2D15, CACNA2D16, CACNA2D17, CACNA2D18, CACNA2D19, CACNA2D20, CACNA2D21, CACNA2D22, CACNA2D23, CACNA2D24, CACNA2D25, CACNA2D26, CACNA2D27, CACNA2D28, CACNA2D29, CACNA2D30, CACNA2D31, CACNA2D32, CACNA2D33, CACNA2D34, CACNA2D35, CACNA2D36, CACNA2D37, CACNA2D38, CACNA2D39, CACNA2D40, CACNA2D41, CACNA2D42, CACNA2D43, CACNA2D44, CACNA2D45, CACNA2D46, CACNA2D47, CACNA2D48, CACNA2D49, CACNA2D50, CACNA2D51, CACNA2D52, CACNA2D53, CACNA2D54, CACNA2D55, CACNA2D56, CACNA2D57, CACNA2D58, CACNA2D59, CACNA2D60, CACNA2D61, CACNA2D62, CACNA2D63, CACNA2D64, CACNA2D65, CACNA2D66, CACNA2D67, CACNA2D68, CACNA2D69, CACNA2D70, CACNA2D71, CACNA2D72, CACNA2D73, CACNA2D74, CACNA2D75, CACNA2D76, CACNA2D77, CACNA2D78, CACNA2D79, CACNA2D80, CACNA2D81, CACNA2D82, CACNA2D83, CACNA2D84, CACNA2D85, CACNA2D86, CACNA2D87, CACNA2D88, CACNA2D89, CACNA2D90, CACNA2D91, CACNA2D92, CACNA2D93, CACNA2D94, CACNA2D95, CACNA2D96, CACNA2D97, CACNA2D98, CACNA2D99, CACNA2D100.

B-YIA1-03

DEVELOPMENT AND VALIDATION OF A MULTI-VARIABLE MODEL FOR REAL-TIME PREDICTION OF CARDIAC ARREST AND OTHER CARDIOVASCULAR (CV) COMPLICATIONS IN HOSPITALIZED PATIENTS WITH COVID-19

Julie K. Shade BS, Ashish N. Doshi MD, PhD, Eric Sung BA, Dan M. Popescu BS, Anum S. Minhas MD, Nisha A. Gilotra MD, Konstantinos N. Aronis MD, Allison G. Hays MD and Natalia A. Trayanova PhD, FHRS

Background: CV manifestations of COVID-19 carry significant morbidity and mortality. Currently, risk prediction for adverse CV events is limited, and existing approaches fail to account for the dynamic course of the disease.

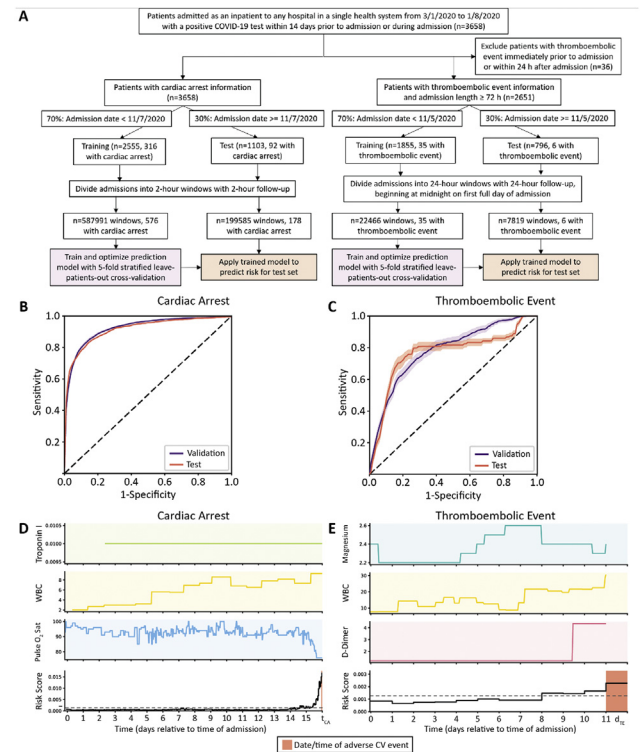
Objective: To develop and validate the COVID-HEART predictor, a novel continuously-updating risk prediction technology, to forecast CV complications in hospitalized patients with COVID-19.

Methods: Vital sign, laboratory, and electrocardiographic data from 2555 and 1855 COVID-19 patients were used to train COVID-HEART to predict cardiac arrest and imaging-confirmed thromboembolic events, respectively. To assess the predictor's performance in the face of rapidly changing clinical treatment guidelines, it was tested on 1103 and 796 patients hospitalized after the end of data collection for the development set (Fig.1A).

Results: In testing, the COVID-HEART predictor achieved areas under the receiver operating characteristic curve (AUROCs) of 0.906 and 0.768, sensitivities of 0.788 and 0.833, and specificities of 0.890 and 0.818 for prediction of cardiac arrest and thromboembolic events, respectively (Fig.1B-C). The respective median test early warning times were 20.5 and 36 hours. Over 20 iterations of temporally-divided testing, the respective mean AUROCs were 0.920 (95% CI: 0.916-0.923) and 0.765 (95% CI: 0.743-0.787).

Conclusion: COVID-HEART is fully transparent and can thus identify predictive features for each outcome derived from clinical data inputs (Fig.1D-E). It is anticipated to provide tangible clinical

decision support in triaging patients and optimizing resource use, with its potential clinical utility extending beyond COVID-19.



ABSTRACT B-YIA2:

Young Investigator Competition - Basic Finalists

Wednesday, June 30, 2021

10:30 am - 11:30 am

B-YIA2-01

MECHANO-ARRHYTHMOGENICITY IS ENHANCED IN LATE REPOLARISATION DURING ISCHEMIA AND DRIVEN BY A TRPA1-, CALCIUM-, AND REACTIVE OXYGEN SPECIES-DEPENDENT MECHANISM

Breanne Ashleigh Cameron BS and T. Alexander Quinn PhD

Background: Cardiac dyskinesia during ischemia results in arrhythmias via mechanically-induced changes in electrophysiology ('mechano-arrhythmogenicity'). While cellular mechanisms of mechano-arrhythmogenicity are unknown, ischemic alterations in voltage-Ca²⁺ dynamics may create a vulnerable period (VP) for mechano-arrhythmogenicity during late repolarisation.

Objective: Determine cellular mechanisms of mechano-arrhythmogenicity in ischemia and define the importance of the VP.

Methods: Rabbit LV myocytes were paced at 1Hz and rapidly stretched (10-18% increase in sarcomere length over ~110ms) during diastole or the VP in control (CTL) or simulated ischemic (SI) conditions. Drugs were used to buffer Ca²⁺ (BAPTA), stabilise ryanodine receptors (dantrolene), block mechano-sensitive TRPA1 (HC-030031) or K_{ATP} channels (glibenclamide), or to chelate (NAC), block (DPI), or increase (fluorophore photoexcitation) reactive oxygen species (ROS) production. Voltage-Ca²⁺ dynamics were simultaneously monitored by dual fluorescence imaging with a single camera-optical splitter system to assess the VP (= Ca²⁺ transient - action potential duration). Diastolic Ca²⁺ was measured with ratiometric imaging.

Results: The VP was longer in SI than CTL (146±7 vs 54±8ms; n=50 cells, N=6 rabbits; p<0.0001). Mechano-arrhythmogenicity